THE EQUILIBRIUM, KINETIC, AND THERMODYNAMIC PARAMETERS OF THE ADSORPTION OF THE FLUORIDE ION ON TO SYNTHETIC NANO SODALITE ZEOLITE

Davoud Balarak,[a] Ferdos Kord Mostafapour,[a] Edris Bazrafshan,[a,b] Amir Hossein Mahvi[b,c,*]

Zahedan and Tehran, Iran

ABSTRACT: The equilibrium, kinetic, and thermodynamic parameters of the adsorption of the fluoride ion (F) on to synthetic nano sodalite zeolite (SNSZ) was studied in a batch system. The SNSZ was characterized by scanning electron microscopy (SEM), X-ray fluorescence (XRF), X-ray diffraction (XRD), and Fourier transform infrared spectroscopy (FTIR) techniques. The experimental data were analyzed by the Langmuir, Freundlich, Redlich-Peterson, Koble-Corrigan, and Temkin isotherm models. The equilibrium data fitted well to the Langmuir model with a maximum adsorption capacity of 25.44 mg/g at 298 K. The pseudo-second-order kinetic model best described the adsorption process. The results proved that the SNSZ was an effective adsorbent for removal of F from aqueous solution. Thermodynamic parameters including the Gibbs free energy (ΔG), enthalpy (ΔH), and entropy (ΔS) were also calculated. These parameters indicated that the adsorption of F on to SNSZ was feasible, spontaneous, and endothermic in nature.

Keywords: Adsorption isotherm; Fluoride; Kinetics; Synthetic nano sodalite zeolite; Thermodynamics.

INTRODUCTION

The fluoride ion (F) is a natural mineral which is present in many foods as well as in drinking water and wastewater.[1-4] Although the use of F topically has been recommended for the prevention of dental caries, F is not an essential element and is not necessary for the development of healthy bones and teeth.[5] A high intake of F can lead to a number of adverse health effects including dental and skeletal fluorosis and a lowering of the IQ in children.[6,7] While the World Health Organization set in 1984 and reaffirmed in 1993 a guideline of 1.5 mg F/L (1.5 ppm) as a "desirable" upper limit, it also allows countries to set country standards, their own national standards or local guidelines.[8,9] Lower country standards have been set of 0.6 mg/L in Senegal, West Africa.[10] and of 1 mg/L in India, with a rider to the Indian limit of the "lesser the fluoride the better, as fluoride is injurious to health."[10] The removal of excessive F from drinking water is a vital for preserving health.

Many methods for the removal of excessive F from aqueous solutions have been investigated in recent years including. adsorption,[11-15] ion exchange,[16] precipitation,[17] electrodialysis,[18] nanofiltration,[19] and ultrafiltration.[20] Considerable attention has been devoted to the study of different types of low-cost materials for F adsorption from aqueous solution such as hydrated

[a]Health Promotion Research Center, Zahedan University of Medical Sciences, Zahedan, Iran; [b] School of Public Health, Tehran University of Medical Sciences, Tehran, Iran; [c]Center for Solid Waste Research, Institute for Environmental Research, Tehran University of Medical Sciences, Tehran, Iran; *For correspondence: Assistant Professor Amir Hossein Mahvi, Center for Solid Waste Research, Institute for Environmental Research, Tehran University of Medical Sciences, Tehran, Iran; E-mail: ahmahvi@yahoo.com.

cement,[21] *Lemna minor*,[22] *Azolla filiculiodes*,[23] canola,[15] calcite,[24] amorphous alumina,[25] red mud,[26] and montmorillonite.[27]

The aim of the present study was to evaluate the feasibility of using synthetic nano sodalite zeolite for the removal of F from aqueous solutions.

MATERIALS AND METHODS

Synthesis of sodalite zeolite: The synthetic nano sodalite zeolite (SNSZ) was provided by the hydrothermal crystallization method using sodium metasilicate ($Na_2O_3Si{\cdot}5H_2O$) and sodium aluminate ($NaAlO_2$) as sources of silica and aluminum, respectively. In a standard synthesis, solution A was prepared by dissolving 18.235 g $Na_2O_3Si{\cdot}5H_2O$ (43% H_2O, 29% Na_2O, 28% SiO_2) in 8 mL double distilled water at 80ºC. Solution B was prepared by dissolving 3.097 g NaOH in 12 mL double distilled water and this solution was then used for solving 1.837 g of $NaAlO_2$. Then, solution A was added to solution B drop wise under vigorous stirring and stirring was continued for 1 hr until hydrothermicity was achieved. The molar composition of the above reactants was as follows: 1.0 Al_2O_3: 3.8 SiO_2: 2.1 Na_2O: 50 H_2O. Subsequently, the above gel was transferred to Teflon lined stainless steel autoclaves and heated at 100ºC for 20 hr under static conditions. At the end of the process, the product was separated via centrifuge (5,000 rpm), washed several times with double distilled water until the pH value of the solution was about 8.0, and dried overnight at 80ºC.

The specific surface area of SNSZ was determined by the BET method using the Gemini 2357 of Micrometrics Co. Scanning electron microscopy (SEM) of the SNSZ were carried out using a (Philips, Eindhoven) scanning microscope equipped with an energy-dispersive X-ray (EDX) (Seron Technologies Inc., Korea [South]). The FTIR spectra (Nicolet 5700 instrument, Thermo Corp, USA) were recorded in the range of 400– 4000 cm^{-1} in order to detect the sodalite functional groups.

Adsorption experiments: All chemicals (NaF, HCl, and NaOH) and reagents (SPADNS reagent and $ZrOCl_2.8H_2O$) used were of analytical reagent grade and were purchased from Merck Co. All glassware and sample bottles were soaked in diluted HNO_3 solution for 24 hr and washed three times with deionized water. The NaF (Merck) was used for the preparation of the standard F stock solution. The required concentration of F solution was prepared by appropriate dilutions of the stock solutions. The pH of the solutions was adjusted to the desired value with 0.1 M HCl and NaOH solutions.

The batch experiment was carried out to measure the adsorption characteristics of F by the SNSZ. The SNSZ (0.3 g) was added to 100 mL of synthetic F solutions of varying concentration (10–100 mg/L). After equilibrium, the samples were filtered and the filtrate was then analyzed for residual F concentration. The experiments were performed in duplicate. 1 mL of $ZrOCl_2.8H_2O$ and 1 mL SPADNS was added into prepared samples. The sample was measured by spectrophotometer in λ_{max}=570 nm. All experiments were performed at a pH equal to 7.

RESULTS AND DISCUSSION

Characterization of synthetic nano sodalite zeolite: The characterization of the SNSZ was done using scanning electron microscopy (SEM), X-ray fluorescence (XRF), X-ray diffraction (XRD), and Fourier transform infrared spectroscopy (FTIR) techniques.

The SEM image of the particles is shown in Figure 1, which shows the morphology of the synthesized zeolite with a small particle size in the range of 30–80 nm.

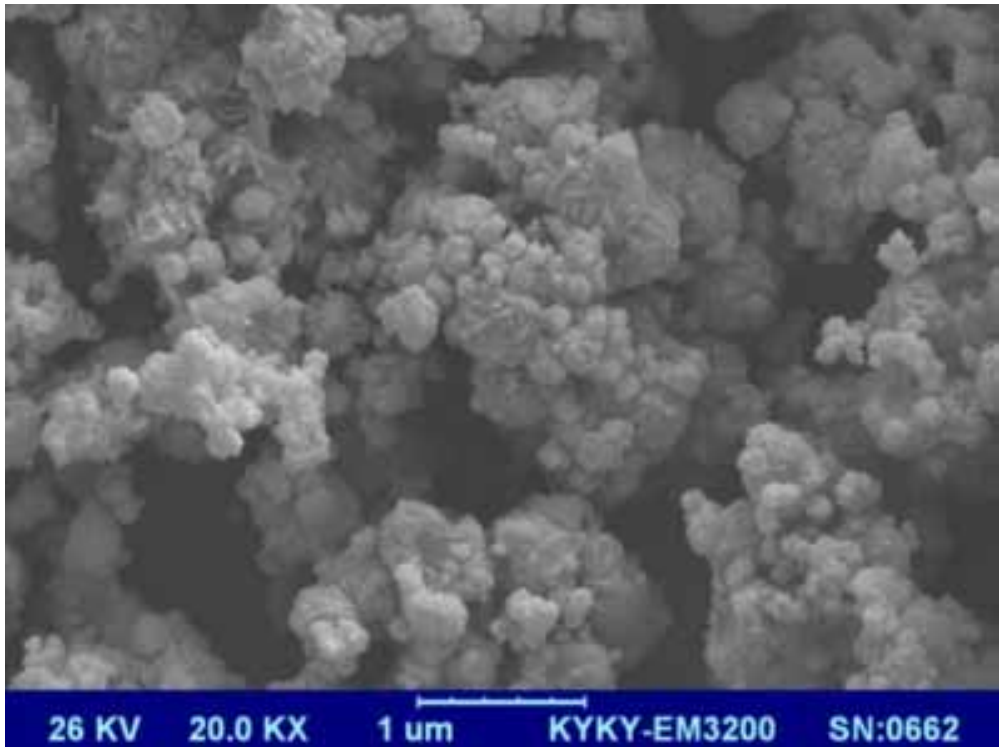

Figure 1. Scanning electron micrograph of sodalite zeolite

The specific surface area is related to the number of active adsorption sites on the SNSZ. The specific surface area of the SNSZ was determined to be 214.5 m^2/g.

The chemical composition of the zeolite was determined by XRF and it includes: 72.6% w/w SiO_2, 15.48% Al_2O_3, 3.24% Na_2O, 3.09% K_2O, 2.48% CaO, 0.98% MnO, 0.84% Fe_2O_3, 0.67% MgO, 0.28% P_2O_5, 0.19% SO_3, and 0.16% TiO_2.

The XRD powder pattern of the SNSZ is presented in Figure 2. The crystallization products matched the characteristic peaks of the SNSZ at 2θ values of 14.1º, 22.5º, 31.9º, and 34.7º that were reported by Buhl, suggesting successful synthesis of sodalite nanozeolite with a good crystalline structure.

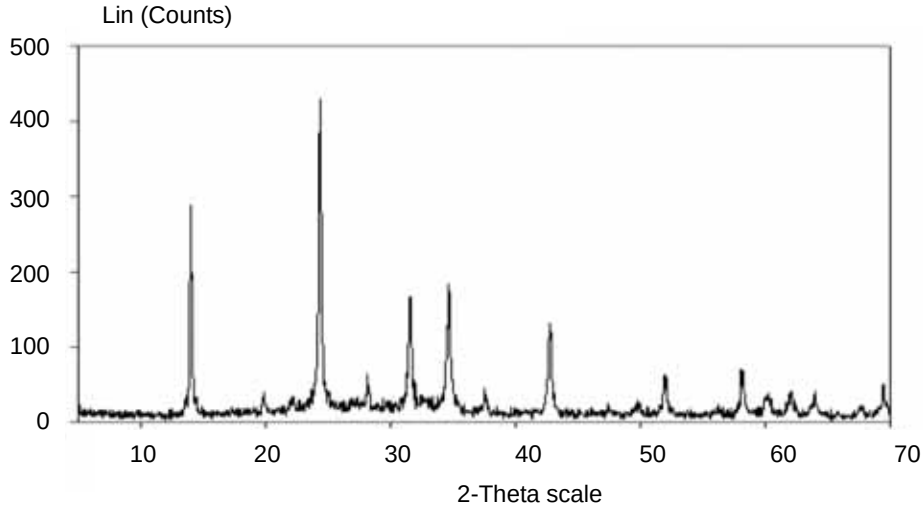

Figure 2. X-ray diffraction of synthesized sodalite zeolite

The sodalite structure has come under scrutiny by means of the FTIR technique as shown in Figure 3. The appropriate crystallization of the zeolitic product is indicated by the sharpness of the band located at 717.6 cm^{-1}, matching the vibration of the Al-O fragment, and the strong broad band at 947.1 cm^{-1} related to the T–O band (T = silica or aluminum).[28] The peak at 1645.4 cm^{-1} is related to the bending vibration of free water. The strong broad band at 3471.2 cm^{-1} indicates the stretching of water molecules adsorbed on OH groups.[29,30]

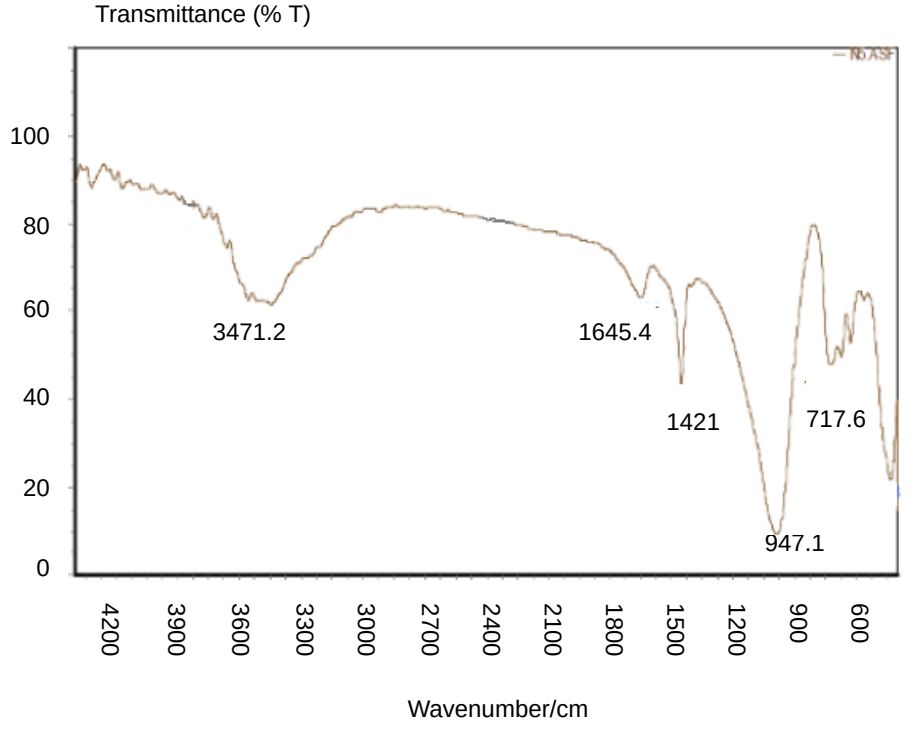

Figure 3. FTIR spectrum of sodalite zeolite

Adsorption isotherms: The experiments to determine the adsorption isotherms were performed with an adsorbent amount of 3 g/L at pH 5. The important parameter in designing the absorption system is the prediction of the adsorption capacity. This can be obtained by analyzing the isotherm data. The equations of isotherms are shown in Table 1.

Table 1. The equations of different isotherms[31-33]

Model	a Isotherm equation
Langmuir	$\frac{1}{q_e} = \left(\frac{1}{q_m K_L} \times \frac{1}{C_e}\right) + \frac{1}{q_m}$
Freundlich	$\text{Log } q_e = \frac{1}{n} \log C_e + \ln K_F$
Redlich-Peterson	$\text{Ln} \frac{A C_e}{q_e - 1} = g \ln C_e + \ln B$
Koble-Corrigan	$\frac{1}{q_e} = \frac{1}{A C_e^n} + \frac{B}{A}$
Tempkin	$q_e = B_1 \ln (k_t) + B_1 \ln (C_e)$

The isotherm parameters and the coefficients of determination (R^2) are listed in Table 2. All the values of R^2 in Table 2 were bigger than 0.85 except for the Freundlich and Temkin models so the three isotherms with R^2 values >0.85, Langmuir, R-Peterson, and Koble-Corrigan, were used to fit the experimental data. This showed that the adsorption process might be a homogeneous adsorption. As shown in Table 2, the constants of K_L, q_m, and K_F were all increased with increasing temperature. These results indicated that F can be easily taken up by SNSZ from aqueous solutions.

The Langmuir constant K_L indicates the affinity for the binding of F. A high K_L value indicates a high affinity. From Table 2, the monolayer or maximum adsorption capacity of SNSZ (q_m), increased as the temperature increased. The values of q_m obtained were 21.18, 25.44, and 28.36 mg/g at 273, 298, 323 K, respectively.

The obtained values of 1/n ($0.1<1/n<1$) indicated a higher adsorb ability for F at all the temperatures studied. The results indicate that as the temperature increased, the ability of the SNSZ to adsorb F also increased.

Examination of the data showed that two isotherms (Redlich-Peterson and Koble-Corrigan) were appropriate descriptions of the data for F adsorption over the concentration ranges studied. The constants g and n were near to 1, and these indicate the isotherms were approaching the Langmuir form.

Table 2. Isotherm parameters for fluoride ion adsorption on to SNSZ

		Temperature (K)		
		273	298	323
Langmuir	q_m (mg/g)	21.18	25.44	28.36
	K_L (L/mg)	0.284	0.325	0.376
	R_L	0.597	0.684	0.749
	R^2	0.998	0.997	0.998
Freundlich	K_F (mg/g)	3.95	4.56	4.87
	1/n	0.211	0.284	0.314
	R^2	0.824	0.819	0.808
Temkin	A (L/g)	12.45	15.46	17.84
	B	1.745	2.234	2.645
	R^2	0.804	0.786	0.815
Redlich-Peterson	A	14.22	18.34	21.46
	B	1.841	2.283	2.457
	g	0.692	0.745	0.792
	R^2	0.924	0.948	0.953
Koble-Corrigan	A	8.144	9.871	11.32
	B	0.152	0.292	0.413
	n	0.382	0.483	0.527
	R^2	0.973	0.959	0.976

Adsorption kinetics: The adsorption kinetics data are one the most important areas for understanding the mechanism of the adsorption and for assessing the performance of the adsorbents. Different kinetic models including the pseudo-first-order, pseudo-second-order, and intra-particle diffusion models were applied for the experimental data to predict the adsorption kinetics.

The pseudo-first-order equation can be written as follows:[34]

$$\text{Log } (q_e - q_t) = \log q_e - \frac{k_1 t}{2.3}$$

where q_e (mg/g) and q_t (mg/g) are the amounts of F adsorbed at equilibrium and at time t, respectively, k_1 (min^{-1}) is the pseudo-first-order rate constant. A straight line of $\ln(q_e-q_t)$ versus t suggests the applicability of this kinetic model, and q_e and k_1 can be determined from the intercept and slope of the plot, respectively.

The pseudo-second-order model is in the following form:[35]

$$\frac{t}{q} = \frac{1}{k_2 q_e^2} + \frac{t}{q_e}$$

where k_2 (g/mg min) is the rate constant of the second-order equation. The plot of t/q_t versus t should give a straight line if the pseudo-second-order kinetic model is applicable and q_e and k_2 can be determined from the slope and intercept of the plot, respectively.

The intraparticle diffusion equation is expressed as:[36]

$$q_e = kt^{½} + C$$

where k (mg/g $min^{1/2}$) is the rate constant of intraparticle diffusion model. The values of k and c can be determined from the slope and intercept of the straight line of q_t versus $t^{1/2}$, respectively.

For evaluating the kinetics of F-SNSZ interactions, the pseudo-first-order, the pseudo-second-order, and the intra-particle diffusion models were used to fit the experimental data.

The pseudo-first-order rate constant k_1 and the value of q_e were calculated from the plot of $\ln(q_e–q_t)$ versus t, and the results are given in Table 3. The correlation coefficient (R^2) is relatively too low which may be indicative of a bad correlation. In addition, the q_e cal determined from the model is not in a good agreement with the experimental value of the q_e exp. Therefore, the adsorption of F on to SNSZ is not suitable for the first-order reaction.

From Table 3, the value of C obtained from the intraparticle diffusion model is not zero, and the correlation coefficient is not satisfactory. Therefore, intraparticle diffusion may not be the controlling factor in determining the kinetics of the process.

The linear plot of t/q_t versus t for the pseudo-second-order kinetic model is shown in Figure 4. The pseudo-second-order rate constant k_2 and the value of q_e cal were determined from the model and the results are presented in Table 3. The value of the correlation coefficient is very high (R^2>0.997) and the calculated q_e cal value is closer to the experimental q_e exp value.

In view of these results, the pseudo-second-order kinetic model provided a good correlation for the adsorption of F on to SNSZ in contrast to the pseudo-first-order and the intra particle diffusion models.

Table 3. Kinetic parameters for the adsorption of the fluoride ion (F) on to SNSZ at various concentrations of F

C_0 (mg F/L)	q_e exp (mg/g)	Kinetic models		
		Pseudo-first-order		
		K_1	q_e	R^2
10	3.24	0.125	2.417	0.789
20	6.32	0.246	5.226	0.804
50	14.35	0.324	11.74	0.823
100	25.16	0.538	19.85	0.817
		Pseudo-second-order		
		K_2	q_e	R^2
10	3.24	0.095	3.511	0.997
20	6.32	0.068	6.742	0.998
50	14.35	0.041	15.26	0.998
100	25.16	0.019	26.72	0.999
		Intraparticle diffusion		
		k	C	R^2
10	3.24	0.152	1.251	0.835
20	6.32	0.194	1.844	0.859
50	14.35	0.237	2.529	0.814
100	25.16	0.296	3.438	0.866

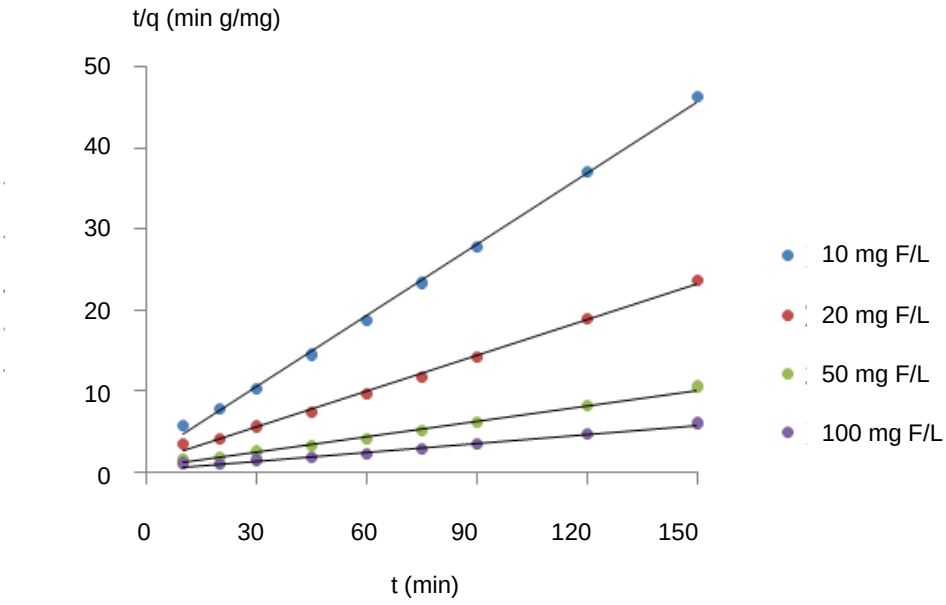

Figure 4. Pseudo-second order kinetics of fluoride (F) adsorption

Thermodynamic parameters: In engineering practice, entropy and energy factors should be considered in order to determine what processes will occur spontaneously. The Gibbs free energy change, ΔG^o, indicates the degree of spontaneity of the adsorption process and higher negative value reflects a more energetically favorable adsorption. The Gibbs free energy change of adsorption is defined as: [37]

$$\Delta G^o = -R\,T\,Ln\,K$$

where R is the universal gas constant (8.314 J/molK), T is the absolute temperature (K), and K is the distribution coefficient. The K value was calculated using following equation:[23]

$$K = \frac{q_e}{C_e}$$

The enthalpy change, (ΔH), and the entropy change, (ΔS), of adsorption were estimated from the following equation:[34]

$$\Delta G^o = \Delta H^o - T\,\Delta S^o$$

This equation can be written as:[37]

$$\text{Ln (K)} = \frac{\Delta S^o}{R} - \frac{\Delta H^o}{R\,T}$$

The values of ΔG^o, ΔH^o, and ΔS^o for the adsorption of F on to SNSZ at different temperatures are given in Table 4.

Table 4. Thermodynamic parameters of adsorption of 2-CP on to rice straw.

Temperature (K)	ΔG° (KJ/mol)	ΔH° (kJ/mol)	ΔS° (J/mol K)
273	–3.51		
298	–1.85	4.18	11.52
323	–0.264		

The negative values of ΔG^o in the temperature range of 273–323 K indicates that the adsorption process is feasible and spontaneous. In addition, the increase in the magnitude of ΔG^o at higher temperatures shows that there is an increase in the spontaneity of the process with increased temperature. Thus, adsorption is more favored at higher temperatures. The positive value of ΔH^o confirms the endothermic nature of the adsorption which is also supported by the increase in the value of the F uptake with the rise in temperature. The positive values of ΔS^o shows the increasing randomness at the solid/liquid interface during the adsorption of F on to SNSZ.

CONCLUSION

In this study, the ability of SNSZ to bind F was tested using the equilibrium, kinetic, and thermodynamic aspects. Five isotherm models were used to express the sorption phenomenon of the sorbate. The equilibrium data were well described by the Langmuir model. The kinetics of F adsorption on to SNSZ were examined using the pseudo-first-order, pseudo-second-order, and intraparticle diffusion models. The results indicated that the pseudo-second-order equation provided the best correlation for the sorption data. The negative value of ΔG^o confirmed the spontaneous nature of the adsorption process. The positive value of ΔS^o showed the increased randomness at the solid-solution interface during adsorption and the positive value of ΔH^o indicated the adsorption process was endothermic.

REFERENCES

1 Boldaji MR, Mahvi AH, Dobaradaran S, Hosseini SS. Evaluating the effectiveness of a hybrid sorbent resin in removing fluoride from water. International Journal of Environmental Science and Technology 2009;6(4):629-32

2 Rahmani A. Rahmani K, Dobaradaran, S., Mahvi AH, Mohamadjani R, Rahmani H, Child dental caries in relation fluoride and some inorganic constituents in drinking water in Arsanjan, Iran. Fluoride 2010;43(3):179-86.
3 Dobaradaran S, Fazelinia F, Mahvi AH, Hosseini SS. Particulate airborne fluoride from an aluminium production plant in Arak, Iran. Fluoride 2009;42(3):228-32.
4 Nouri J, Mahvi AH, Babaei A, Ahmadpour E. Regional pattern distribution of groundwater fluoride in the Shush aquifer of Khuzestan County, Iran. Fluoride 2006;39(4):321-5.
5 Scientific Committee on Health and Environmental Risks (SCHER). Opinion of critical review of any new evidence on the hazard profile, health effects, and human exposure to fluoride and the fluoridating agents of drinking water. Brussels, Belgium: Directorate General for Health and Consumers, European Commission; 2011 May 16. pp. 2-4.
6 Karimzade S, Aghaei M, Mahvi AH. Investigation of intelligence quotient in 9–12-year-old children exposed to high- and low-drinking water fluoride in west Azerbaijan province, Iran. Fluoride 2014;47(1):9-14
7 Aghaei M, Karimzade S, Yaseri M, Khorsandi H, Zolfi E, Mahvi AH. Hypertension and fluoride in drinking water: case study from west Azerbaijan, Iran. Fluoride 2015;48(3):252-8.
8 WHO. Fluoride in drinking-water: background document for development of WHO guidelines for drinking-water quality. WHO/SDE/WSH/03.04.96, English only. Geneva: WHO; 2004. Available from: http://www.who.int/water_sanitation_health/dwq/chemicals/fluoride.pdf
9 WHO. Guidelines for drinking-water quality: incorporating first addendum to third edition. Vol 1. Recommendations. Geneva; World Health Organization; 2006. Available from: http://helid.digicollection.org/en/p/printable.html.
10 Susheela AK. A treatise on fluorosis. 3rd ed. Delhi: Fluorosis Research and Rural Development Foundation; 2007. pp. 15-6.
11 Bazrafshan E, Balarak D, Panahi AH, Kamani H, Mahvi AH. Fluoride removal from aqueous solutions by cupricoxide nanoparticles. Fluoride 2006;49(3 Pt 1):233-44.
12 Chen N, Zhang Z, Feng C, Sugiura N, Li M, Chen R. Fluoride removal from water by granular ceramic adsorption. Journal of Colloid and Interface Science 2010;348:579-84.
13 Haghighat GA, Dehghani MH, Nasseri S, Mahvi AH, Rastkari N. Comparison of carbon nonotubes and activated alumina efficiencies in fluoride removal from drinking water. Indian Journal of Science and Technology 2012;5(23):2432-5.
14 Balarak D, Mahdavi Y, Bazrafshan E, Mahvi AH, Esfandyari Y. Adsorption of fluoride from aqueous solutions by carbon nanotubes: determination of equilibrium, kinetic, and thermodynamic parameters. Fluoride 2016;49(1):71-83.
15 Zazouli MA, Mahvi AH, Mahdavi Y, Balarak D. Isothermic and kinetic modeling of fluoride removal from water by means of the natural biosorbents sorghum and canola. Fluoride 2015;48(1):37-44.
16 Meenakshi S, Viswanathan N. Identification of selective ion-exchange resin for fluoride sorption. J Colloid Interface Sci 2007;308:438-50.
17 Sujana MG, Thakur RS, Das SN, Rao SB, Defluorination of waste waters. Asian J Chem 1997;4:561-70.
18 Zeni M, Riveros R, Melo K, Primieri R, Lorenzini S. Study on fluoride reduction in artesian well-water from electrodialysis process. Desalination 2005;185:241-4.
19 Simons R. Trace element removal from ash dam waters by nanofiltration and diffusion dialysis. Desalination 1993;89:325-41.
20 Guo L, Hunt BJ, Santsci PH. Ultrafiltration behavior of major ions (Na, Ca, Mg, F, Cl, and SO_4) in natural waters. Water Res 2001;35(6):1500-8.
21 Kagne S, Jagtap S, Dhawade P, Kamble SP, Devotta S, Rayalu SS. Hydrated cement: a promising adsorbent for the removal of fluoride from aqueous solution. J Hazard Mater 2008;154:88-95.
22 Zazouli MA, Balarak D, Karimnezhad F, Khosravi F. Removal of fluoride from aqueous solution by using of adsorption onto modified *Lemna minor:* adsorption isotherm and kinetics study. Journal of Mazandaran University Medical Sciences 2014;23(109):208-17.

23 Zazouli MA, Mahvi AH, Dobaradaran S, Barafrashtehpour M, Mahdavi Y, Balarak D. Adsorption of fluoride from aqueous solution by modified *Azolla filiculoides*. Fluoride 2014;47(4):349-58.
24 Yang M, Hashimoto T, Hoshi N, Myoga H. Fluoride removal in a fixed bed packed with granular calcite. Water Res 1999;33:3395-402.
25 Li YH, Wang S, Cao A, Zhao D, Zhang X, Xu C, Z. Luan Z, et al. Adsorption of fluoride from water by amorphous alumina supported on carbon nanotubes. Chem Phys Lett 2001;350:412-6.
26 Genc H, Tjell JC, McConchie D, Schuiling RD. Adsorption of arsenate from water using neutralized red mud. J Colloid Interface Sci 2003;264:327-34.
27 Tor A. Removal of fluoride from an aqueous solution by using montmorillonite. Desalination 2006;201:267-76.
28 Rahmani SH, Azizi SN, Asemi N. Application of synthetic nanozeolite sodalite in drug delivery. International Current Pharmaceutical Journal 2016;5(6):55-8
29 Esfandian H, Fakhraee H, Azizi A. Removal of strontium Ions by synthetic nano sodalite zeolite from aqueous solution. International Journal of Engineering 2016;29(2);160-9.
30 Vadapalli VR, Gitari WM, Ellendt A, Petrik LF, Balfour G. Synthesis of zeolite-P from coal fly ash derivative and its utilisation in mine-water remediation. South African Journal of Science 2010;106:62-8.
31 Kumar E, Bhatnagar A, Kumar U, Sillanpaa M. Defluoridation from aqueous solutions by nano-alumina: characterization and sorption studies. J Hazard Mater 2011;186(2-3):1042-9.
32 Balarak D. Kinetics, Isotherm and thermodynamics studies on bisphenol A adsorption using barley husk. International Journal of Chem Tech Research 2016;9(5):681-90.
33 Bhaumik R, Mondal NK, Das B, Roy P, Pal, KC, Das C, et al. Eggshell powder as an adsorbent for removal of fluoride from aqueous solution: equilibrium, kinetic and thermodynamic studies. J Chem 2012;9:1457-80.
34 Ma W, Ya FQ, Han M, Wang RJ. Characteristics of equilibrium, kinetics studies for adsorption of fluoride on magnetic-chitosan particle. J Hazard Mater 2007;143:296-302.
35 Srivastav AL, Singh PK, Srivastava V, Sharma YC. Application of a new adsorbent for fluoride removal from aqueous solutions. J Hazard Mater 2013;263:342-52.
36 Balarak D, Jaafari J, Hassani G, Mahdavi Y, Tyagi I, Agarwal S, Gupta VK. The use of low-cost adsorbent (Canola residues) for the adsorption of methylene blue from aqueous solution: Isotherm, kinetic and thermodynamic studies. Colloids and Interface Science Communications. Colloids and Interface Science Communications 2015;7:16-9.
37 Balarak D, Mahdavi Y, Bazrafshan E, Mahvi AH. Kinetic, isotherms and thermodynamic modeling for adsorption of acid blue 92 from aqueous solution by modified *Azolla filicoloides*. Fresenius Environmental Bulletin 2016;25(5):1321-30.